Molecular BioSystems

PAPER

Cite this: *Mol. BioSyst.*, 2017, 13, 2379

Modelling the propagation of a dynamical signature in gene expression mediated by the transport of extracellular microRNAs†

Alexis Grau Ribes,[ab] Yannick De Decker,[ab] Claude Gérard*[c] and Laurence Rongy[ab]

Received 19th August 2017,
Accepted 18th September 2017

DOI: 10.1039/c7mb00509a

rsc.li/molecular-biosystems

Extracellular microRNAs (miRNAs) carried by exosomes can play a key role in cell-to-cell communication. Deregulation of miRNA expression and exosome secretion have been related to pathological conditions such as cancer. While it is known that circulating miRNAs can alter gene expression in recipient cells, it remains unclear how significant the dynamical impact of these extracellular miRNAs is. To shed light on this issue, we propose a model for the spatio-temporal evolution of the protein expression in a cell tissue altered by abnormal miRNA expression in a donor cell. This results in a nonhomogeneous cellular response in the tissue, which we quantify by studying the range of action of the donor cell on the surrounding cells. Key model parameters that control the range of action are identified. Based on a model for a heterogeneous cell population, we show that the dynamics of gene expression in the tissue is robust to random changes of the parameter values. Furthermore, we study the propagation of gene expression oscillations in a tissue induced by extracellular miRNAs. In the donor cell, the miRNA inhibits its own transcription which can give rise to local oscillations in gene expression. The resulting oscillations of the concentration of extracellular miRNA induce oscillations of the protein concentration in recipient cells. We analyse the nonmonotonic spatial evolution of the oscillation amplitude of the protein concentration in the tissue which may have implications for the propagation of oscillations in biological rhythms such as the circadian clock.

1 Introduction

MicroRNAs (miRNAs) are short sequences of 18–24 nucleotides that repress gene expression in a post-transcriptional manner.[1] Hundreds of different miRNAs are present in mammals and target most mammalian messenger RNAs (mRNAs).[2] MiRNAs are important regulators for multiple biological processes such as cell differentiation,[3] cell growth and tumorigenesis,[4–6] cancer cell migration,[7] morphogenesis,[8] the immune system,[9] the links between inflammation and cell transformation,[10,11] or the control of biological rhythms.[12] Moreover, they can confer robustness to gene expression.[13,14]

In a multicellular organism, cell-to-cell communication is crucial for the proper development and function of the organism as well as for the preservation of homeostasis. Besides direct cell-to-cell contacts and secreted signals through soluble factors, *i.e.* inflammatory mediators, cytokines or hormones, an additional mechanism of intercellular communication mediated by extracellular vesicles (EVs) such as exosomes and micro-vesicles has recently been discovered.[15,16] Exosomes are nano-vesicles containing proteins, mRNAs and miRNAs protected by a lipid bilayer. They are produced by multiple cell types and can be secreted to neighbouring or distant cells by transport of EVs through body fluids.[17]

Secretion of extracellular miRNAs by a donor cell, through EVs, can alter gene expression profiles in a recipient cell.[15] Indeed, several studies showed that miRNAs can be transferred to immune, cancer or endothelial cells allowing for a modification of their gene expression levels.[18–20] These modes of cell-to-cell communication are also important under physiological conditions such as neuronal development and neuron excitability.[21–23] EVs and miRNAs are also key regulators under pathological conditions such as inflammation and cancers.[24–26] In this context, it was shown that breast cancer cells could affect their surrounding microenvironment by secreting exosomes that contain extracellular miRNAs, thereby promoting tumorigenesis.[27] Cancer cells can thus create an oncogenic field around them by secreting extracellular miRNAs.[27] However, little is known about the dynamical consequences of the presence of extracellular miRNAs on the gene expression levels in the recipient cells. In particular,

[a] *Nonlinear Physical Chemistry Unit, Faculté des Sciences, Université libre de Bruxelles (ULB), Brussels, Belgium. E-mail: lrongy@ulb.ac.be; Fax: +32 (0)2 650 5767; Tel: +32 (0)2 650 5699*
[b] *Center for Nonlinear Phenomena and Complex Systems (CENOLI), Université libre de Bruxelles (ULB), Brussels, Belgium*
[c] *de Duve Institute, Université Catholique de Louvain (UCL), Brussels, Belgium. E-mail: claude.gerard@uclouvain.be*

† Electronic supplementary information (ESI) available. See DOI: 10.1039/c7mb00509a

the parameters that could affect the range of action of an extracellular miRNA are still poorly understood.

Previous theoretical studies involving miRNAs have accounted for the kinetic signatures of their modes of action[28,29] and the dynamics arising as a result of miRNA-mediated translation repression. Other mathematical models including the miRNA Let-7, a key tumor suppressor, were proposed to describe the dynamics of gene regulatory networks involved in the development of lung cancer or in an epigenetic switch linking inflammation to cell transformation.[30,31] The role played by miRNAs in the dynamics arising in competing endogenous (ceRNA) networks has been studied with the help of minimal mathematical models.[32,33] In addition, numerous experimental and theoretical studies based on reaction-diffusion models pertained to the spatiotemporal analysis of the formation of morphogen gradients, which is particularly crucial during embryonic development.[34–37] However, to the best of our knowledge, the spatio-temporal models describing the dynamics arising as a consequence of extracellular miRNA propagation are still missing.

In this context, we propose a minimal spatio-temporal mathematical model based on partial differential equations for the regulation of the level of a protein output in recipient cells by the propagation of an extracellular miRNA. Our study aims at better defining the parameters that could control the range of action of extracellular miRNAs (see Section 2.1.3), which can be of great importance for the oncogenic field generated by cancer cells in their microenvironment. We will further show how an extracellular miRNA could play a role in synchronising gene expression in a tissue.

Moreover, several studies indicate that miRNAs are also key components for the regulation of the circadian clock in mammals.[12,38] Indeed, miR-132 and miR-219, two brain-specific miRNAs, modulate the circadian rhythms in the suprachiasmatic nucleus, which is the master circadian clock in mammals and miR-122 in the liver was also identified as a modulator of the negative feedback loop driving the circadian clock.[12,39] In addition, the expression levels of some circulating miRNAs were shown to oscillate with a circadian period, suggesting a role for extracellular miRNAs in the regulation of the circadian clock.[40] To illustrate the potential impact of extracellular miRNAs in the regulation of circadian rhythms within a cell tissue, we extend the model by considering that, in the donor cell, the secreted miRNA is embedded in a negative feedback loop, which is the core regulatory motif that allows for the generation of circadian rhythms. The latter model will allow us to analyze the dynamical consequences of an oscillating extracellular miRNA on the protein output in recipient cells and will shed light on how a dynamical signature of gene expression in a donor cell could be propagated to recipient cells.

2 Results

2.1 Minimal model for miRNA propagation in a cell tissue: effect on protein output

2.1.1 Description of the model. We propose a minimal model in order to focus on the effects arising from miRNA propagation and to separate them from those due to the non-linear dynamics inherent to the gene regulatory network present in the cells. The system includes a single type of messenger RNA whose synthesis is activated by a transcription factor (TF). This RNA encodes the synthesis of a protein (Prot) and, by forming a complex (C) with RNA, a miRNA regulates the expression of this protein. One cell in the middle of the tissue shows abnormal expression of miRNA and its influence on the protein expression in neighbouring cells will be studied.

This cell (Cell 0), exhibiting abnormal miRNA expression, may represent a progenitor cell surrounded by parenchyma cells or may correspond to a deregulated, *i.e.* cancer cell. All the other cells are considered identical so that the spatial concentration profiles of the different species are symmetric around Cell 0 (Fig. 1). Because of this geometry, two- or three-dimensional simulations are not expected to give more information on the dynamics of the system than one-dimensional (1-D) ones. We thus model the spatio-temporal evolution of concentrations only in the cells at the right side of Cell 0 using a symmetrical boundary condition. This assumption is consistent with other theoretical works that model the diffusion of miRNAs or morphogens through a 1-D tissue.[41–43] We have shown that the conclusions for the 1-D and 2-D systems are qualitatively the same (see supplementary material S1, ESI†).

The cells can communicate with each other by the transport of miRNA. We suppose that other species do not travel from one cell to another. The loading of miRNAs into exosomes, the secretion and dissemination of these exosomes in the extracellular matrix and their merging with neighbouring cells are modelled by an exchange term with an effective transport coefficient (D). The spatio-temporal evolution of miRNA, RNA, C and Prot is described in each cell by four differential equations, one for the concentration of each species:

$$\frac{\partial \mathrm{miRNA}}{\partial t} = v_{\mathrm{smiRNA}} - k_1 \cdot \mathrm{miRNA} \cdot \mathrm{RNA} + k_2 \cdot \mathrm{C} + k_{\mathrm{dC}} \cdot \mathrm{C} - k_{\mathrm{dmiRNA}} \cdot \mathrm{miRNA} + D\frac{\partial^2 \mathrm{miRNA}}{\partial x^2}, \quad (1)$$

$$\frac{\mathrm{dC}}{\mathrm{d}t} = k_1 \cdot \mathrm{miRNA} \cdot \mathrm{RNA} - k_2 \cdot \mathrm{C} - k_{\mathrm{dC}} \cdot \mathrm{C}, \quad (2)$$

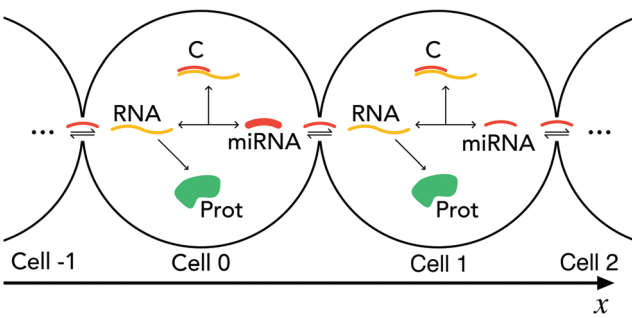

Fig. 1 Scheme of the minimal model. RNA encodes the synthesis of Prot. RNA and miRNA can form C, an inhibitory complex that prevents Prot synthesis. MiRNA is able to propagate to neighbouring cells where it inhibits the synthesis of Prot. Cell 0 has an abnormal synthesis rate of miRNA compared to the other cells and the 1-D tissue is symmetric around Cell 0.

$$\frac{\mathrm{dRNA}}{\mathrm{d}t} = v_{\mathrm{sRNA}} \cdot \left(\frac{\mathrm{TF}^4}{K^4 + \mathrm{TF}^4}\right) - k_1 \cdot \mathrm{miRNA} \cdot \mathrm{RNA} + k_2 \cdot \mathrm{C} - k_{\mathrm{dRNA}} \cdot \mathrm{RNA}, \quad (3)$$

$$\frac{\mathrm{dProt}}{\mathrm{d}t} = k_{\mathrm{sProt}} \cdot \mathrm{RNA} - k_{\mathrm{dProt}} \cdot \mathrm{Prot}. \quad (4)$$

The definition, value and units of the variables and parameters are presented in Table 1. Most terms of the evolution equations rest on the mass action law such as the formation and dissociation of the complex C (first two terms of eqn (2)), the synthesis of the protein (first term of eqn (4)) and the degradation of each species. We consider that only RNA is degraded in the complex, C, and miRNA is released in its free form again (fourth term of eqn (1)). A Hill function is used for the RNA synthesis term, which is controlled by the oligomerization of TF, with a coefficient of cooperativity equal to 4 (first term of eqn (3)). Oligomerization of transcription factors in the regulation of gene expression has been shown experimentally.[44]

2.1.2 Estimation of the parameter values of the model. The calibration of the model was based on experimental measurements for Prot, RNA and miRNA abundance[45,46] and for the rate constants for Prot and RNA degradation.[47] RNA abundance can vary from 1 to 100 copies per cell. Basing our calculations on 10 copies per cell of 0.01 mm diameter, we estimate a concentration of 10^{-2} nM. We therefore use parameter values for the messenger RNA to obtain a concentration of 10^{-2} nM for the basal concentration of RNA. Since protein abundance can be a thousand times higher than their corresponding RNA copy number (varying from 100 to 100 000 protein copies per cell), the parameter values for the protein were chosen to obtain approximately 10 nM as the basal concentration of the protein ($\sim$13 nM in the first model, $\sim$7 nM in the model describing oscillations). The average half-life durations of RNAs and proteins are 9 h and 46 h, respectively.[47] The corresponding degradation rates are $k_{\mathrm{dRNA}} = 0.077\ \mathrm{h}^{-1}$ and $k_{\mathrm{dProt}} = 0.015\ \mathrm{h}^{-1}$, respectively. The values of v_{sRNA}, TF, K, k_1, k_2 and k_{sProt} were chosen to fit the basal concentration of messenger RNA and protein. A similar approach was used for the expression of microRNAs. The abundance of most expressed microRNAs can vary from 100 to 2000 copies per cell.[46] We therefore chose 1000 copies per cell in our model as a representative number and fixed v_{smiRNA} and k_{dmiRNA} accordingly. Another important part of the calibration of the model was the evaluation of the effective transport coefficient. Experimental measurements of the velocity of exosomes in the cell, through the membrane and in the extracellular matrix, have been performed and it can vary from 10^{-3} to 1 $\mu\mathrm{m}^2\ \mathrm{s}^{-1}$ (corresponding to 10^{-5} and $10^{-2}\ \mathrm{mm}^2\ \mathrm{h}^{-1}$).[48] In our study, we have varied the effective transport coefficient between 10^{-5} and 1 $\mathrm{mm}^2\ \mathrm{h}^{-1}$.

The condition at the right boundary of the tissue is no-flux. These equations are integrated numerically using finite differences in space and a fourth-order Runge–Kutta time integration scheme. Initial conditions are the stationary solution when the synthesis rate of miRNA in Cell 0 is the same as in other cells (see Table 1). The simulation is then initiated by setting the synthesis rate of miRNA in the donor cell (Cell 0) to a higher value than in other cells. The tissue is 100-cell long on each side of Cell 0 and the distance between the centres of two cells is $\mathrm{d}x = 0.01$ mm in agreement with experimental data showing that 10 μm is a representative size for the diameter of epithelial cells.[49] The corresponding time step is $\mathrm{d}t = 10^{-5}$ h. The effect of the size of the tissue on the dynamics of the system will be discussed below.

2.1.3 Range of action of the donor cell. For all the parameter values studied here, a steady regime is reached where stationary gradients of concentrations are observed in the tissue (Fig. 2A and B). The miRNA concentration is maximum around Cell 0 due to its abnormal production and then decreases monotonically through the tissue. In contrast, RNA and protein concentrations increase monotonically. We define the horizontal dotted line in Fig. 2 as a threshold of protein concentration below which the cellular response changes. As a consequence of the miRNA gradient throughout the tissue, a certain number of cells

Table 1 Variable and parameter definitions, values, initial conditions (i.c.) and units in the minimal model

Symbol	Definition	Value	Units
Variables			
miRNA	MicroRNA concentration	1.0 (i.c.)	nM
RNA	Messenger RNA concentration	0.01 (i.c.)	nM
C	Complex form by RNA and miRNA concentration	0.01 (i.c.)	nM
Prot	Protein concentration	13.3 (i.c.)	nM
Parameters			
v_{smiRNA}	Synthesis rate of miRNA (in all cells except Cell 0)	10^{-1}	nM h^{-1}
v_{sRNA}	Synthesis rate of RNA	20	nM h^{-1}
TF	Transcription factor concentration	10	nM
K	Michaelis constant for the activation of RNA synthesis by the transcription factor	10	nM
k_1	Rate constant for the binding between miRNA and RNA	10^3	$\mathrm{nM}^{-1}\ \mathrm{h}^{-1}$
k_2	Rate constant for the dissociation of C	10^{-3}	h^{-1}
k_{dmiRNA}	Rate constant for miRNA degradation	10^{-1}	h^{-1}
k_{dRNA}	Rate constant for RNA degradation	0.077	h^{-1}
k_{dC}	Rate constant for RNA degradation in the complex C	1	h^{-1}
k_{sProt}	Rate constant for protein synthesis	20	h^{-1}
k_{dProt}	Rate constant for protein degradation	0.015	h^{-1}
D	Effective transport coefficient of miRNA	10^{-5}–1	$\mathrm{mm}^2\ \mathrm{h}^{-1}$

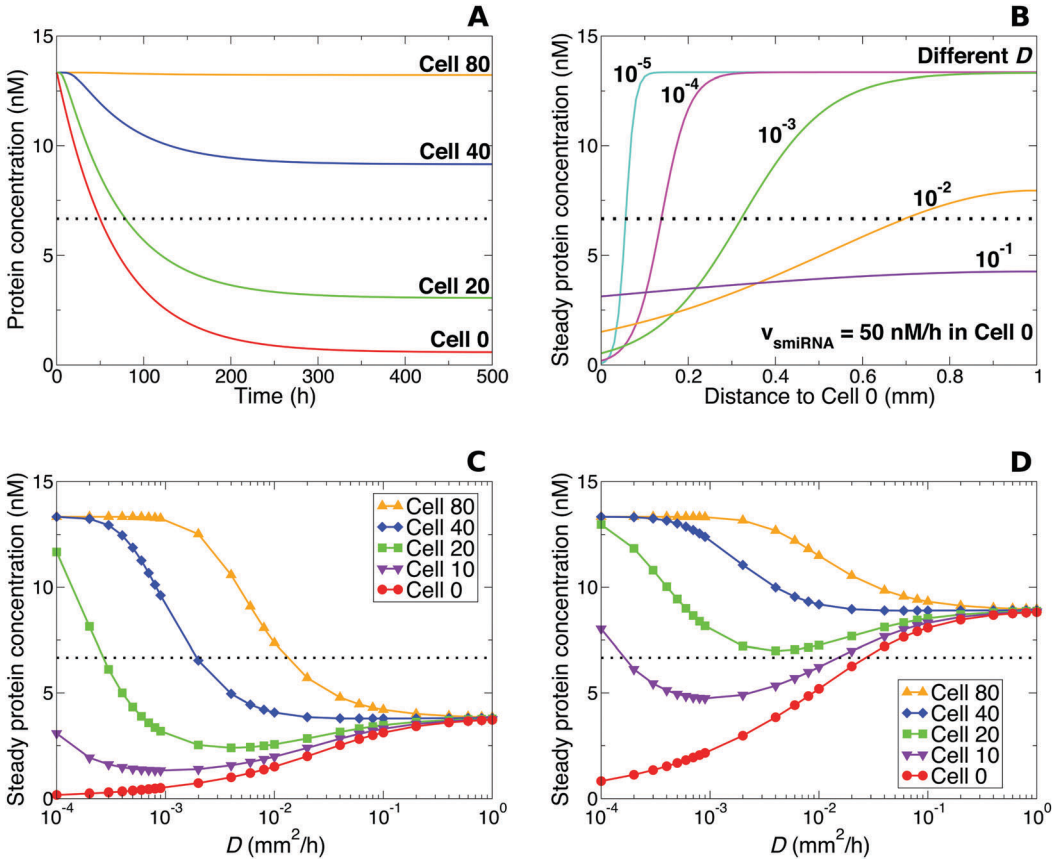

Fig. 2 Stationary profiles of protein concentration. (A) Temporal evolution of the protein concentration in five different cells with $D = 10^{-3}$ mm^2 h^{-1} and $v_{\mathrm{smiRNA}} = 50$ nM h^{-1} in Cell 0. (B) Stationary profiles of protein concentration in the tissue for several transport coefficients in mm^2 h^{-1}. (C and D) Protein concentration at the steady state in some cells as a function of the transport coefficient of miRNA. (C) $v_{\mathrm{smiRNA}} = 50$ nM h^{-1} in Cell 0 and (D) $v_{\mathrm{smiRNA}} = 10$ nM h^{-1} in Cell 0. The dotted line is an arbitrary threshold of protein concentration below which the cellular response changes. The tissue is 100-cell long.

have their protein concentration below the threshold which allows us to define therefore the range of action of Cell 0 as the distance between Cell 0 and the farthest of such cells. We set the threshold arbitrarily at half the basal protein concentration in the tissue. We have, however, verified that changing this threshold does not qualitatively change our conclusions. The range of action (ROA) is defined in terms of the distance to Cell 0 (x_{r}) as

$$\mathrm{ROA} \equiv x_{\mathrm{r}} \text{ such as } \mathrm{Prot}(x_{\mathrm{r}}) = \frac{\mathrm{Prot}_{\mathrm{basal}}}{2}. \quad (5)$$

An analytical approximation for the range of action can be obtained from eqn (1)–(4). Adding eqn (1) and (2), we obtain an evolution equation for miRNA which has only three parameters: the synthesis rate of miRNA, the rate constant for miRNA degradation and the transport coefficient. Using no-flux boundary condition at both the ends of the tissue and imposing a different synthesis rate of miRNA in Cell 0 than in the rest of the tissue, the stationary profile of miRNA concentration in the tissue can be obtained analytically. The stationary concentration of the other variables in each cell can be obtained by substitution into eqn (2)–(4). After imposing that the range of action must be zero when $D = 0$ and considering that the binding between miRNA and RNA is much more favourable than their dissociation ($k_1 \gg 1 \gg k_2$) and that the length of the tissue is much larger than the distance between two cells ($L \gg \mathrm{d}x$), the final expression reads

$$\mathrm{ROA} = \sqrt{\frac{D}{k_{\mathrm{dmiRNA}}}} \ln\left[\left(\mathrm{e}^{\mathrm{d}x\sqrt{\frac{D}{k_{\mathrm{dmiRNA}}}}} - 1\right)\frac{\delta v_{\mathrm{s}}}{2}\right] - \frac{\mathrm{d}x}{2}, \quad (6)$$

with

$$\delta v_{\mathrm{s}} = \frac{v^0_{\mathrm{smiRNA}} - v_{\mathrm{smiRNA}}}{v_{\mathrm{smiRNA}}}, \quad (7)$$

where v^0_{smiRNA} and v_{smiRNA} are the synthesis rate of miRNA in Cell 0 and in other cells respectively, and $\mathrm{d}x$ is the distance between two cells. Calculations leading to eqn (6) are shown in the supplementary material S2 (ESI†).

2.1.4 What controls the range of action? As shown in eqn (6), the range of action only depends on the transport coefficient, the synthesis rate of miRNA, the rate constant for miRNA degradation and the distance between the cells. This has been confirmed in numerical simulations where changing the value of the other parameters of the model changes the basal expression of the protein in the tissue only but does not affect the range of action of the donor cell (see supplementary material S3, ESI†).

Fig. 2B shows how the stationary gradient of protein concentration in the tissue varies with the value of the transport coefficient for a given value of the synthesis rate of miRNA. For small values of the transport coefficient, miRNAs do not propagate far in the tissue, the protein gradient is steep and the range of action is small. The cellular response is therefore nonhomogeneous in the tissue. When the transport coefficient is large, miRNA reaches all the cells and the protein concentration is almost uniform. The cellular response is therefore homogeneous in the tissue either below the threshold (see Fig. 2C for a large synthesis rate of miRNA in Cell 0) or above the threshold (see Fig. 2D for a small synthesis rate of miRNA in Cell 0).

The fact that transport can act as a sink term of miRNA for the donor cell and those close to it, and as a miRNA source term for cells further away in the tissue explains the dependence of the steady protein concentration as a function of the transport term. In Cell 0, miRNA concentration decreases and protein concentration increases with the transport coefficient while the opposite is true in the cells far away in the tissue. In intermediate cells, the protein concentration goes through a minimum as a function of D. Enhancing the transport indeed increases miRNA (decreases the protein) concentration until D reaches a critical value where increasing it further dilutes miRNA in the tissue and therefore acts as a miRNA sink term for those intermediate cells, thereby increasing the protein concentration (see Fig. 2C and D).

Interestingly, we found that the rate constant for miRNA degradation (k_{dmiRNA}) has the exact opposite influence on the range of action as D which cannot be seen straightforwardly from eqn (1)–(4) but can be identified in eqn (6). Multiplying D by a factor has the same effect on the range of action as dividing k_{dmiRNA} by the same factor. The influence of both the parameters can thus be analyzed by varying the D/k_{dmiRNA} ratio.

Fig. 3 shows how the range of action depends on D/k_{dmiRNA} and on the synthesis rate of miRNA. Analytical and numerical results show a good general agreement. First, we note that

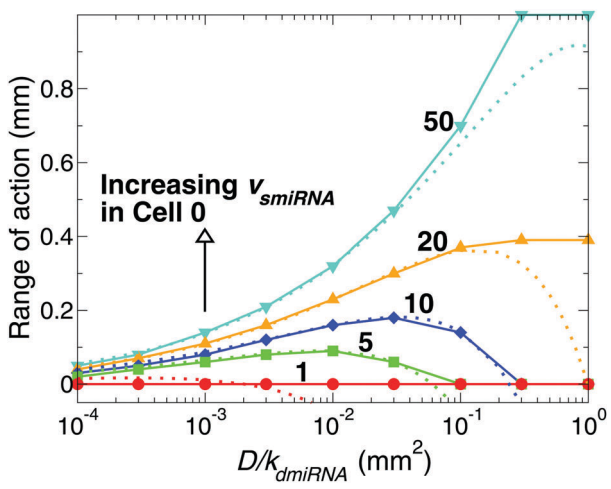

Fig. 3 Parametric dependence of the range of action. Range of action as a function of D/k_{dmiRNA} for different values of the synthesis rate of miRNA in Cell 0 (1, 5, 10, 20 and 50 nM h^{-1} from bottom to top) obtained with numerical simulations (solid lines) and analytical formulation (dotted lines).

increasing the synthesis rate of miRNA in the donor cell at fixed D/k_{dmiRNA} ratio always increases the range of action. When the synthesis rate of miRNA in Cell 0 is not sufficiently large compared with other cells, the range of action is zero regardless of the value of the D/k_{dmiRNA} ratio. There is not enough miRNA produced in Cell 0 to bring the protein concentration below the threshold (see the red line in Fig. 3 where v_{smiRNA} is ten times larger than in the other cells). For intermediate values of the synthesis rate of miRNA in Cell 0, the range of action presents a maximum for intermediate D/k_{dmiRNA} ratio and vanishes at high D/k_{dmiRNA}. This maximum can be understood by the same mechanism explained above based on the competition between increasing the distance of miRNA propagation and diluting it when D/k_{dmiRNA} increases. This maximum will therefore be observed at a larger D/k_{dmiRNA} ratio when the synthesis rate of miRNA in the donor cell increases. From eqn (6), we can find an analytical expression for this maximum. Assuming that the distance where the maximum occurs, $(\mathrm{ROA})_{\max}$, is typically larger than dx, we find

$$\left(\frac{D}{k_{\mathrm{dmiRNA}}}\right)_{\max} = \mathrm{d}x^2\left(\frac{\delta v_{\mathrm{s}}}{2e}\right)^2, \tag{8}$$

$$(\mathrm{ROA})_{\max} \approx \mathrm{d}x\left(\frac{\delta v_{\mathrm{s}}}{2e} - \frac{1}{2}\right), \tag{9}$$

and we see that the position of the maximum range of action only depends on the difference between the synthesis rate of miRNA in the donor cell *versus* the other cells. We can also find in the same limit coordinates for which the range of action is zero:

$$\left(\frac{D}{k_{\mathrm{dmiRNA}}}\right)_0 \approx \mathrm{d}x^2\left(\frac{\delta v_{\mathrm{s}}}{2}\right)^2 = \left(\frac{D}{k_{\mathrm{dmiRNA}}}\right)_{\max} e^2. \tag{10}$$

At sufficiently large D/k_{dmiRNA}, the range of action reaches 0, which corresponds to the case illustrated in Fig. 2D where all the cells are above the threshold at large D. Our analytical formulation predicts a negative value for the range of action at high D/k_{dmiRNA} which means that even Cell 0 is above the threshold for those conditions. The abnormal expression of miRNA in Cell 0 is compensated by a large exchange rate.

For higher values of the synthesis rate of miRNA in Cell 0, since the system is defined by a finite number of cells (here, 100), the cellular response is altered in all the tissue (turquoise line corresponding to the case illustrated in Fig. 2C where at large D, all the cells have their protein concentration below the threshold). This example illustrates the fact that the propagation of miRNA can be limited by the size of the tissue in *in vivo* or in *in vitro* experiments. Finally, we notice that the analytical interpretation fails to reproduce the numerical results at high values of the synthesis rate of miRNA and D/k_{dmiRNA}. This arises from the assumption, in the analytical formulation, that the tissue is very long ($L \gg \mathrm{d}x$) while biological tissues have a finite size.

2.1.5 Protein expression in a tissue with a heterogeneous cell population. Cells from *in vitro* cell culture or from an *in vivo* tissue may be very heterogeneous. This is particularly true in cancer cell populations.[50] To account for such heterogeneity,

we will resort to a model for a heterogeneous cell population where the value of each parameter in each cell is chosen randomly within an interval of ±20% around its mean value (Table 1). The model indicates that the protein concentration at the steady state presents a large variability within the tissue whether miRNA diffuses or not (see Fig. 4A for a low synthesis rate of miRNA in the donor cell). This suggests that protein concentration cannot be homogenised in a heterogeneous cell population only by the transport of miRNA.

We now turn to the situation where one cell has an abnormally large synthesis rate of miRNA. We show here that the concept of range of action discussed in the previous section extends to the case of a heterogeneous cell population. For small transport coefficients, several cells close to Cell 0 have their protein concentration below the threshold because of the large synthesis rate of miRNA in Cell 0 (see the red curve in Fig. 4B). The number of cells with a protein concentration below the threshold depends on the transport coefficient and the synthesis rate of miRNA in Cell 0 as illustrated in Fig. 4C. When there is no diffusion of miRNA, the number of cells below the threshold varies between 0 and 10 from one simulation to another due to natural parameter variability (*cf.* Fig. 4A). We observe a good agreement between the range of action defined in a homogeneous cell population and the number of cells below the threshold in a heterogeneous cell population. This suggests that the range of action is in general robust to random variations in gene expression in the tissue. However, for large values of the transport coefficient and small values of the synthesis rate of miRNA in Cell 0, the range of action fails to describe the dynamics in a heterogeneous cell population. The number of cells below the threshold indeed saturates around a certain value in a heterogeneous cell population, while the range of action goes to zero in a homogeneous cell population for large transport coefficients as explained in the previous section. This can be understood by looking at the protein concentration in a heterogeneous cell population for large D and low v_{smiRNA} (Fig. 2D).

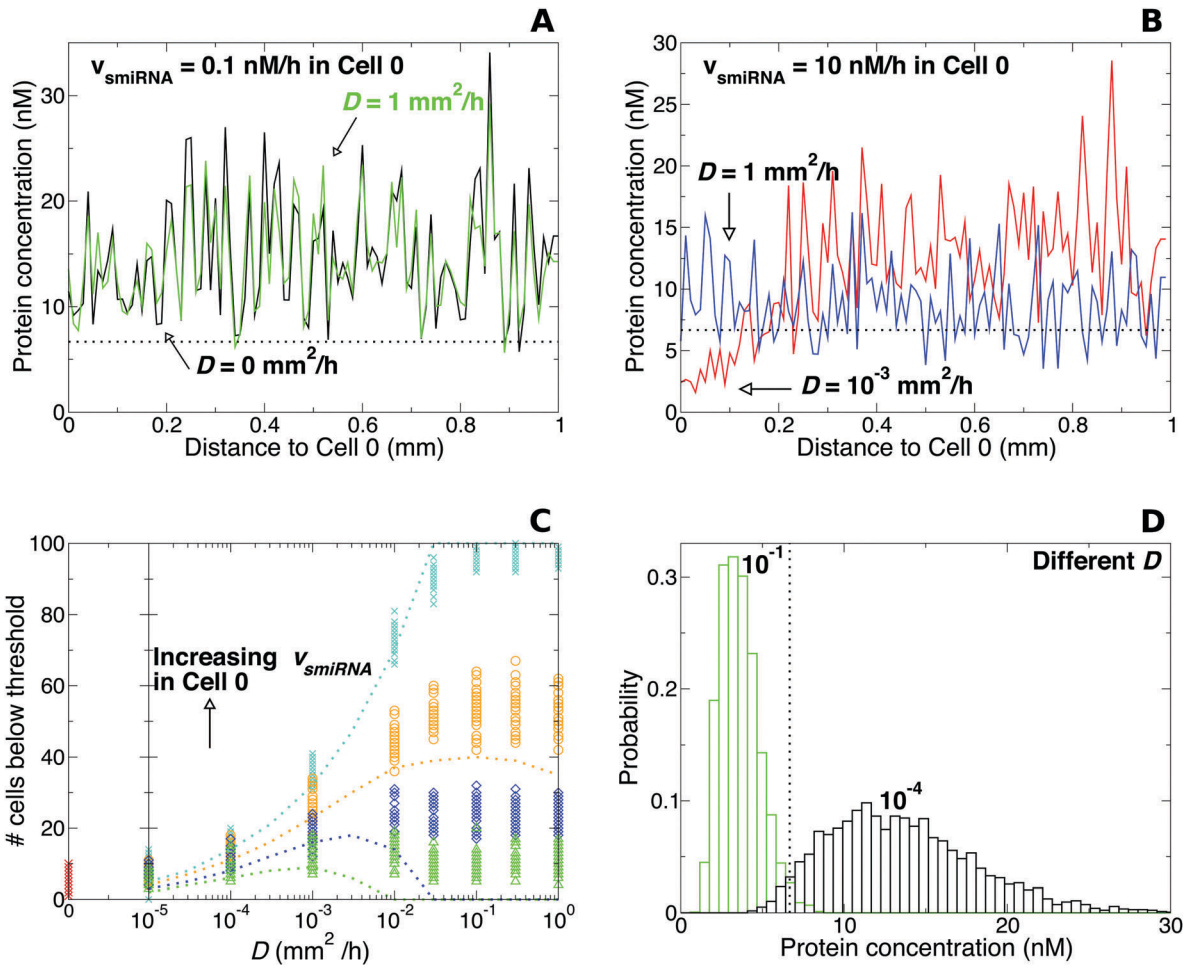

Fig. 4 Robustness of gene expression in a heterogeneous cell population. (A) Protein concentration profiles with (green line) and without (black line) transport of miRNA in the tissue. A random variation of ±20% around the default value is used for each parameter in each cell while v_{smiRNA} = 0.1 nM h^{-1} in Cell 0. (B) Protein concentration profiles in the tissue for two different values of the transport coefficient where v_{smiRNA} = 10 nM h^{-1} in Cell 0. (C) Number of cells in the tissue having their protein concentration below the threshold as a function of D for 4 different values of v_{smiRNA} in Cell 0: 5, 10, 20 and 50 nM h^{-1} from bottom to top. 30 simulations were performed for each value of D and v_{smiRNA}. Dotted lines represent the range of action as a function of D for a homogeneous cell population. (D) Numerical probability distribution of the protein concentration in Cell 25 for two different values of D in mm^2 h^{-1} and v_{smiRNA} = 50 nM h^{-1} in Cell 0 obtained from 3000 simulations. The horizontal dotted line in (A) and (B) and the vertical dotted line in (D) are the defined threshold for cellular response.

The protein concentration is above the threshold in all the tissues but close to its value. Therefore, with random variation in the parameter values, we observe that there is always a certain number of cells below the threshold (see the blue curve in Fig. 4B).

Finally, we calculated the numerical probability distribution of the protein concentration in each cell for different values of the transport coefficient. Fig. 4D shows two probability distributions in Cell 25 for a large synthesis rate of miRNA in Cell 0. The absolute variability of the protein concentration is smaller at large D conferring robustness to the cellular response (above or below the defined threshold).

In conclusion, it is important to notice that only miRNA can be transported in our model and that, although its transport is not enough to smooth out the natural variability in protein concentration, it is at the origin of the propagation of a dynamical signature in the protein expression within a range of action even in a heterogeneous cell population.

2.2 Propagation of temporal oscillations in gene expression by intercellular exchanges of miRNA

2.2.1 Description of the model. As mentioned earlier, miRNAs are involved in many biological processes including biological rhythms.[6,12,51,52] Some miRNAs are embedded in a complex gene regulatory network containing negative or positive feedback loops[53,54] and many miRNAs have been shown to regulate their own transcription.[55] Since miRNAs can move from one cell to another, one might ask how this transport affects the dynamics of gene regulatory networks and, conversely, how these networks influence the transport of miRNA. In this context, we propose a model to study the impact of diffusive miRNAs embedded in a negative feedback loop (NFL) in a donor cell (Cell 0) on the expression of a protein output in neighbouring cells. In Cell 0, one type of miRNA is expressed that can bind with a first messenger RNA (RNA1). This inhibits the synthesis of a protein (Prot1). Prot1 is the transcription factor for a second messenger RNA (RNA2) that encodes the synthesis of another protein (Prot2) which is the transcription factor for the miRNA (Fig. 5). In summary, the miRNA inhibits Prot1 expression and therefore its own transcription. The evolution equations of the concentration of the different species involved in the NFL in Cell 0 are:

$$\frac{\partial \mathrm{miRNA}}{\partial t} = v_{\mathrm{smiRNA}} \cdot \left(\frac{\mathrm{Prot2}^4}{K_2^4 + \mathrm{Prot2}^4}\right) - k_1 \cdot \mathrm{miRNA} \cdot \mathrm{RNA1} + k_2 \cdot \mathrm{C1} + k_{\mathrm{dC1}} \cdot \mathrm{C1} - k_{\mathrm{dmiRNA}} \cdot \mathrm{miRNA} + D\frac{\partial^2}{\partial x^2}\mathrm{miRNA}, \quad (11)$$

$$\frac{\mathrm{dC1}}{\mathrm{d}t} = k_1 \cdot \mathrm{miRNA} \cdot \mathrm{RNA1} - k_2 \cdot \mathrm{C1} - k_{\mathrm{dC1}} \cdot \mathrm{C1}, \quad (12)$$

$$\frac{\mathrm{dRNA1}}{\mathrm{d}t} = v_{\mathrm{sRNA1}} - k_1 \cdot \mathrm{miRNA} \cdot \mathrm{RNA} + k_2 \cdot \mathrm{C1} - k_{\mathrm{dRNA1}} \cdot \mathrm{RNA1}, \quad (13)$$

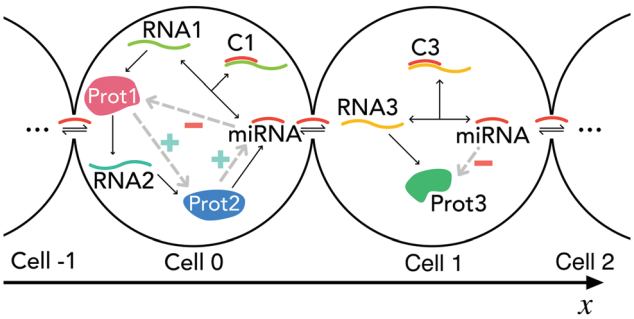

Fig. 5 Scheme of the model for the propagation of temporal oscillations of gene expression. In Cell 0, miRNA is involved in a NFL in which it represses its own transcription. Two proteins and two messenger RNAs are also involved in this loop. In other cells, miRNA regulates the transcription of Prot3. In these cells, miRNA is not involved in a NFL.

$$\frac{\mathrm{dProt1}}{\mathrm{d}t} = k_{\mathrm{sProt1}} \cdot \mathrm{RNA1} - k_{\mathrm{dProt1}} \cdot \mathrm{Prot1}, \quad (14)$$

$$\frac{\mathrm{dRNA2}}{\mathrm{d}t} = v_{\mathrm{sRNA2}} \cdot \left(\frac{\mathrm{Prot1}^4}{K_1^4 + \mathrm{Prot1}^4}\right) - k_{\mathrm{dRNA2}} \cdot \mathrm{RNA2}, \quad (15)$$

$$\frac{\mathrm{dProt2}}{\mathrm{d}t} = k_{\mathrm{sProt2}} \cdot \mathrm{RNA2} - k_{\mathrm{dProt2}} \cdot \mathrm{Prot2}. \quad (16)$$

The definition, value and units of the variables and parameters are presented in Table 2. Hill functions are used for the synthesis of miRNA (first term of eqn (11)) and RNA2 (first term of eqn (15)) where we consider a coefficient of cooperativity equal to 4 between the transcription factors, Prot1 and Prot2, respectively. The other kinetic terms are similar to those in the previous model. The other cells are assumed to produce only one type of messenger RNA (RNA3) which encodes the synthesis of a protein (Prot3). These cells also produce miRNA that inhibits the expression of Prot3. Since this miRNA is the same as that produced in Cell 0, Prot3 expression is also inhibited by miRNA propagating from Cell 0. The evolution equations in cells 1 to 100 read:

$$\frac{\partial \mathrm{miRNA}}{\partial t} = v_{\mathrm{smiRNA}} - k_3 \cdot \mathrm{miRNA} \cdot \mathrm{RNA3} + k_4 \cdot \mathrm{C3} + k_{\mathrm{dC3}} \cdot \mathrm{C3} - k_{\mathrm{dmiRNA}} \cdot \mathrm{miRNA} + D\frac{\partial^2}{\partial x^2}\mathrm{miRNA}, \quad (17)$$

$$\frac{\mathrm{dC3}}{\mathrm{d}t} = k_3 \cdot \mathrm{miRNA} \cdot \mathrm{RNA3} - k_4 \cdot \mathrm{C3} - k_{\mathrm{dC3}} \cdot \mathrm{C3}, \quad (18)$$

$$\frac{\mathrm{dRNA3}}{\mathrm{d}t} = v_{\mathrm{sRNA3}} \cdot \left(\frac{\mathrm{TF}^4}{K_3^4 + \mathrm{TF}^4}\right) - k_3 \cdot \mathrm{miRNA} \cdot \mathrm{RNA3} + k_4 \cdot \mathrm{C3} - k_{\mathrm{dRNA3}} \cdot \mathrm{RNA3}, \quad (19)$$

$$\frac{\mathrm{dProt3}}{\mathrm{d}t} = k_{\mathrm{sProt3}} \cdot \mathrm{RNA3} - k_{\mathrm{dProt3}} \cdot \mathrm{Prot3}. \quad (20)$$

Table 2 Variable and parameter definitions, values, initial conditions (i.c.) and units in the model based on a NFL

Symbol	Definition	Value	Units
Cell 0			
Variables			
miRNA	MicroRNA concentration	0.5 (i.c.)	nM
RNA1	Messenger RNA 1 concentration	0.001 (i.c.)	nM
C1	Inhibitory complex RNA1–microRNA concentration	0.001 (i.c.)	nM
Prot1	Protein 1 concentration	0.5 (i.c.)	nM
RNA2	Messenger RNA 2 concentration	0.6 (i.c.)	nM
Prot2	Protein 2 concentration	0.2 (i.c.)	nM
Parameters			
ν_{smiRNA}	Synthesis rate of miRNA	10	nM h^{-1}
ν_{sRNA1}	Synthesis rate of RNA1	10^{-1}	nM h^{-1}
ν_{sRNA2}	Synthesis rate of RNA2	10^{-3}	nM h^{-1}
K_1, K_2	Michaelis constants for the activation of the synthesis of RNA1 and 2 by the transcription factor (Prot1 and 2)	4	nM
k_1	Rate constant for the binding between miRNA and RNA1	10^3	nM^{-1} h^{-1}
k_2	Rate constant for the dissociation of C1	10^{-3}	h^{-1}
k_{dmiRNA}	Rate constant for miRNA degradation	0.02	h^{-1}
k_{dRNA1}, k_{dRNA2}	Rate constant for RNA1 and RNA2 degradation	0.077	h^{-1}
k_{dC1}	Rate constant for RNA1 degradation in the complex C1	1	h^{-1}
k_{sProt1}, k_{sProt2}	Rate constant for the synthesis of Prot1 and Prot2	50	h^{-1}
k_{dProt1}, k_{dProt2}	Rate constant for Prot1 and Prot2 degradation	0.015	h^{-1}
Other cells			
Variables			
miRNA	MicroRNA concentration	1.0 (i.c.)	nM
RNA3	Messenger RNA3 concentration	0.01 (i.c.)	nM
C3	Inhibitory complex RNA3–microRNA concentration	0.01 (i.c.)	nM
Prot3	Protein 3 concentration	13.3 (i.c.)	nM
Parameters			
ν_{smiRNA}	Synthesis rate of miRNA	10^{-1}	nM h^{-1}
ν_{sRNA3}	Synthesis rate of RNA3	20	nM h^{-1}
TF	Transcription factor concentration	10	nM
K_3	Michaelis constant for the activation of RNA3 synthesis by TF	10	nM
k_3	Rate constant for the binding between miRNA and RNA3	10^3	nM^{-1} h^{-1}
k_4	Rate constant for the dissociation of C3	10^{-3}	h^{-1}
k_{dmiRNA}	Rate constant for miRNA degradation	10^{-1}	h^{-1}
k_{dRNA3}	Rate constant for RNA3 degradation	0.077	h^{-1}
k_{dC3}	Rate constant for RNA3 degradation in the complex C3	1	h^{-1}
k_{sProt3}	Rate constant for the synthesis of Prot3	20	h^{-1}
k_{dProt3}	Rate constant for Prot3 degradation	0.015	h^{-1}
D	Effective transport coefficient of miRNA	10^{-5}–1	mm^2 h^{-1}

This model allows the study of how temporal oscillations of miRNA concentration driven by the NFL in a single cell can propagate in a tissue and how these oscillations influence the protein output in neighbouring cells. Initials conditions are the stationary concentration of each variable of the model without Cell 0.

2.2.2 Temporal dynamics emerging from the NFL in Cell 0. We first focus on the temporal dynamics of the NFL described in eqn (11)–(16) without considering the transport of miRNA. Fig. 6A shows the bifurcation diagram of miRNA concentration as a function of its synthesis rate. Before the Hopf bifurcation (HB), the system reaches a stable steady state characterised by a constant miRNA concentration. At the HB, this branch loses stability (dashed line) and the system presents sustained oscillations. The green lines represent the minima and the maxima of the oscillations of miRNA concentration. Fig. 6B and C show the temporal evolution of the concentrations of miRNA, Prot1 and Prot2 in the system on both the sides of the HB. For small synthesis rates of miRNA, concentrations show damped oscillations before reaching their stationary value. For larger values, the system reaches an asymptotic oscillatory regime where the amplitude and the period of oscillations are constant.

2.2.3 Propagation of gene expression oscillations in the tissue. When miRNA is excreted from the donor cell (Cell 0) and propagates in the tissue, oscillations in gene expression are observed in all the cells reached by the miRNA. Fig. 7A shows the temporal evolution of miRNA concentration in 4 different cells (Cells 1, 10, 20 and 60). The amplitude of the oscillations of miRNA concentration is large in Cell 1 because of its proximity to Cell 0. The amplitude of the oscillations of miRNA concentration decreases with the distance to Cell 0. At some distance to Cell 0, miRNA concentration does not oscillate and remains constant within numerical precision at a value equal to its initial concentration. The oscillations of miRNA concentration induce oscillations of RNA3 and Prot3 concentration. Interestingly, the amplitude of the oscillations of Prot3 concentration is a nonmonotonic function of the distance to Cell 0. The origin of this nonmonotonic dependence is discussed below. We also notice that the shape of the oscillations of Prot3 concentration changes from one cell to another. This shape depends on the ratio between miRNA and RNA3 concentration in each cell. This property is intrinsic to the NFL and is observed in a homogeneous system as well.

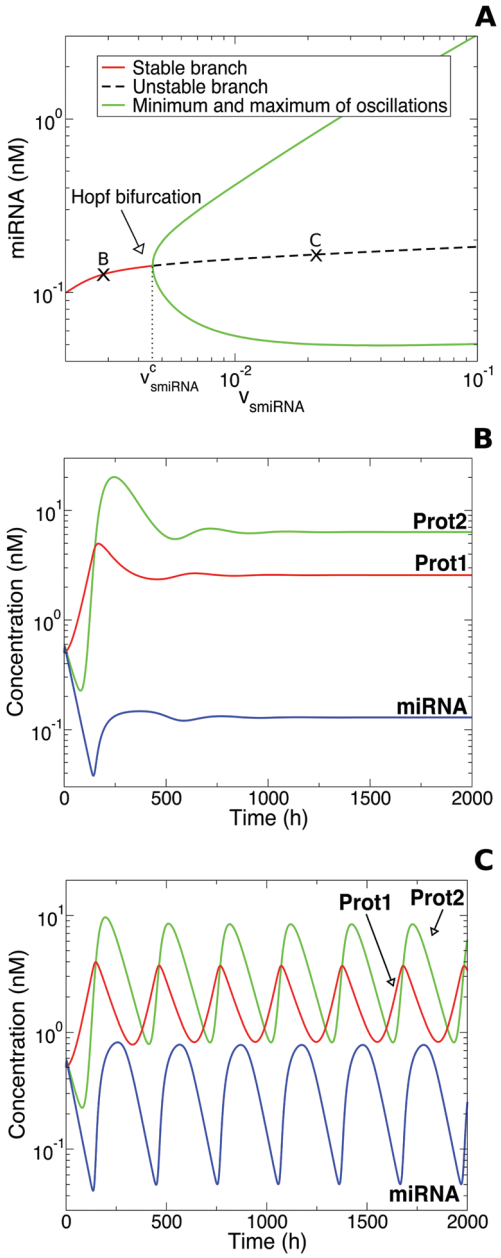

Fig. 6 Temporal dynamics of the miRNA-based NFL. (A) Bifurcation diagram of the miRNA concentration. Before the HB, the red line is the stationary value of miRNA concentration as a function of v_{smiRNA}. After the HB, the stationary state is unstable (dashed line). The green lines are the minima and the maxima of the oscillations as a function of v_{smiRNA}. Temporal evolution of the concentration of miRNA, Prot1 and Prot2 for v_{smiRNA} = 0.003 nM h^{-1} (B) and for v_{smiRNA} = 0.02 nM h^{-1} (C). Other parameter values are as in Table 2.

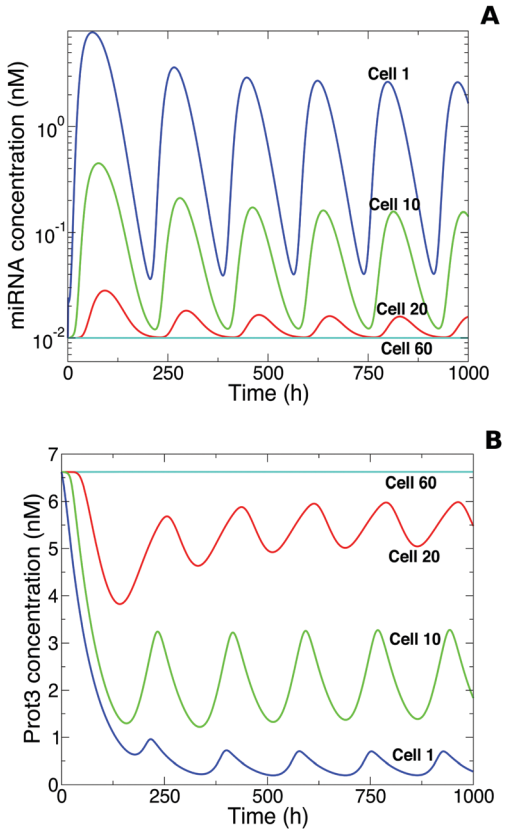

Fig. 7 Propagation of oscillatory behaviour in gene expression induced by an extracellular miRNA. Time evolution of the concentration of miRNA in cells 1, 10, 20 and 60 from top to bottom (A) and of Prot3 in cells 1, 10, 20 and 60 from bottom to top (B). $D = 10^{-4}$ mm^2 h^{-1} and v_{smiRNA} = 10 nM h^{-1} in Cell 0.

2.2.4 What controls the amplitude of gene expression oscillations in the tissue? The spatial evolution of the average concentration of miRNA and Prot3 in the asymptotic oscillatory regime is similar to that of the minimal model: sharp gradients of concentration are observed for small transport coefficients while for large transport coefficients the average concentration is identical in all the cells (Fig. 8A and B). For miRNA concentration, the amplitude of the oscillations decreases with the distance from Cell 0 (as shown in Fig. 8C for different D). By increasing the transport coefficient, oscillations of miRNA concentration can be observed in all the cells of the tissue. The model shows that, unlike miRNA, the amplitude of the oscillations of Prot3 concentration shows a nonmonotonic dependence on the distance from Cell 0 (Fig. 8D). In the cells close to Cell 0, oscillations of Prot3 concentration have small amplitudes because of the high concentration of miRNA in these cells (see the blue curve in Fig. 8E). At large distance from Cell 0, the amplitude of oscillations of miRNA concentration is so small that amplitudes of oscillations of RNA3 and Prot3 concentration are also small (see the red curve in Fig. 8E). The largest oscillations of Prot3 concentration are observed in intermediate cells where the miRNA average concentration is low and where the amplitude of the oscillation of miRNA concentration is large (see the green curve in Fig. 8E). Finally, Fig. 8D shows that the position of the maximum of amplitude in the tissue increases monotonically with the value of the transport coefficient. The model thus predicts a counter-intuitive dynamical behaviour where the influence of the donor cell can be greater on distant cells than on cells in its close proximity.

A displacement of the Hopf bifurcation point arises from the excretion of miRNA from Cell 0, which decreases its local concentration (see Fig. 9A). An increase in the transport coefficient

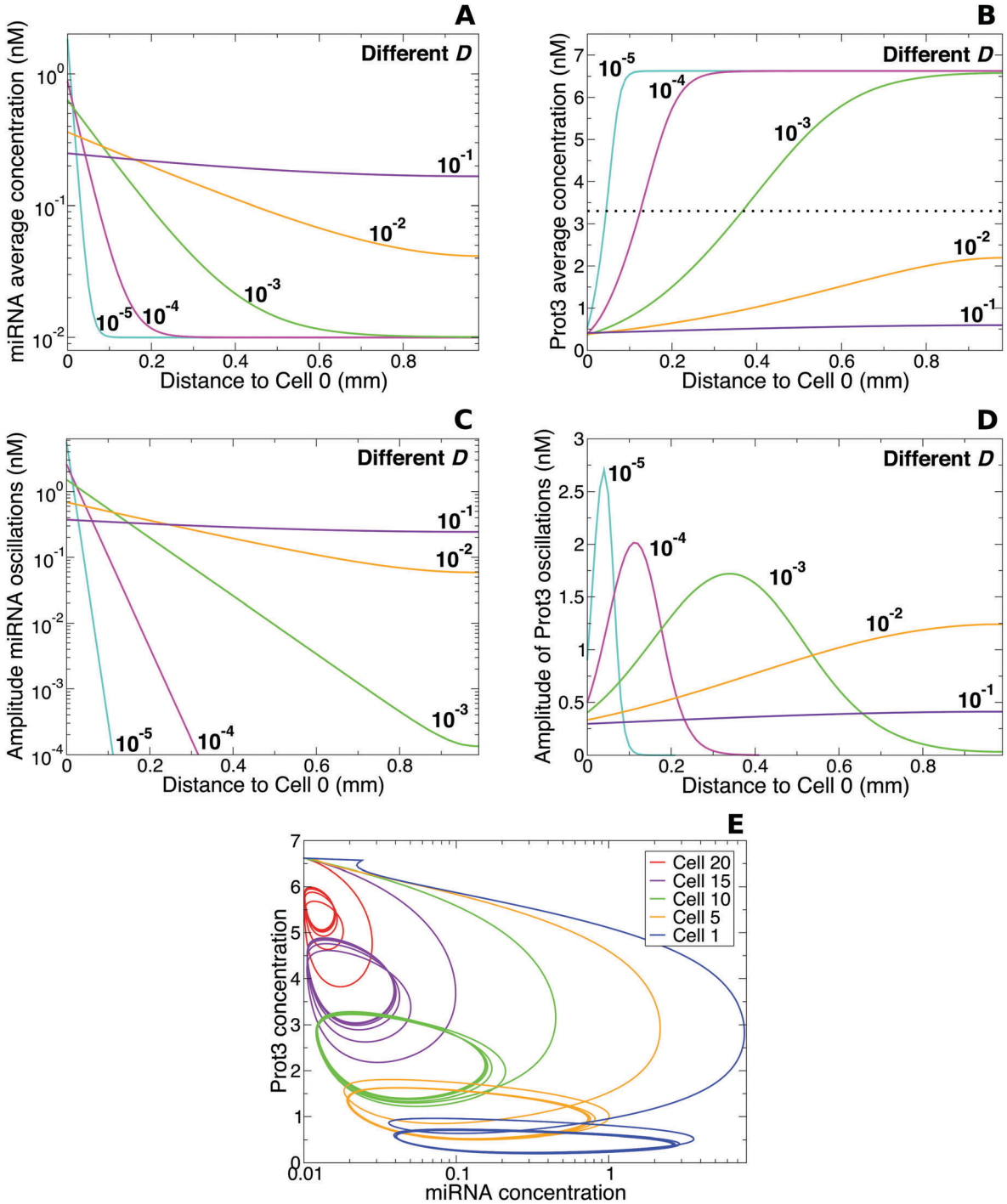

Fig. 8 Influence of the transport coefficient on the amplitude of gene expression oscillations in the tissue. Average concentrations over time of miRNA (A) and Prot3 (B) at the asymptotic oscillatory regime are shown together with the amplitude of the oscillations of miRNA (C) and Prot3 (D) in the tissue for different values of the transport coefficient (in $mm^2\ h^{-1}$). (E) Trajectories in the phase plane defined by miRNA and Prot3 concentrations in nM for different cells with $D = 10^{-4}\ mm^2\ h^{-1}$ and $v_{smiRNA} = 10\ nM\ h^{-1}$ in Cell 0.

means the synthesis rate of miRNA in Cell 0 must be increased to compensate for the loss of miRNA. The amount of miRNA synthesised in Cell 0 is thus an important control parameter as shown in Fig. 9B. By varying this parameter, one can change the amplitude of oscillations, displace the maximum of the amplitude of Prot3 oscillations and also destroy oscillations. Indeed, when the synthesis rate of miRNA in Cell 0 is small, there is no oscillation in the tissue and the system reaches a steady state while at larger values sustained oscillations of Prot3 concentration appear in the tissue. The amplitude of these oscillations increases with the value of the synthesis rate of miRNA in Cell 0 and saturates at large values.

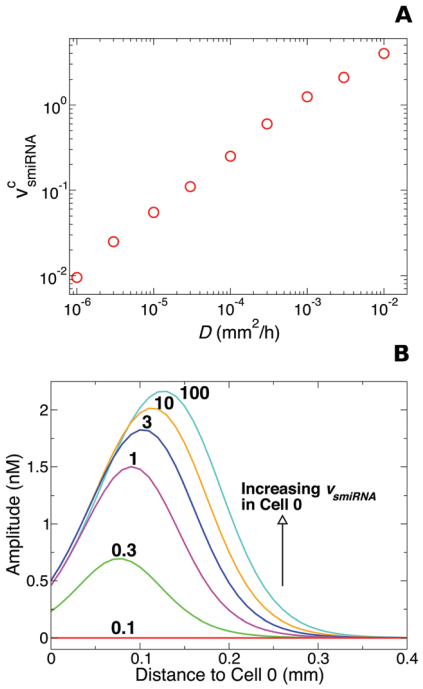

Fig. 9 Influence of the synthesis rate of miRNA in Cell 0 on the dynamics of the system. (A) Displacement of the Hopf bifurcation as a function of D. v^c_{smiRNA} is the critical value of the synthesis rate of miRNA at the HB (in nM h^{-1}). (B) Amplitude of the oscillations of Prot3 concentration in each cell of the tissue for different values of v_{smiRNA} in Cell 0 and for $D = 10^{-4}$ mm^2 h^{-1}.

3 Discussion

Because they allow for cell-to-cell communication between cancer cells and normal host cells, it has been suggested that extracellular miRNAs are crucial components for the regulation of the tumor microenvironment.[27,56–58] In that context, we proposed a first minimal spatio-temporal mathematical model for the propagation of an extracellular miRNA from a donor cell to recipient cells with the aim of highlighting the qualitative dynamical changes induced by miRNA on the gene expression profiles in recipient cells (see the scheme in Fig. 1). The model shows that miRNA produced by the donor cell can significantly reduce the protein expression in recipient cells. An increase in the transport coefficient of the extracellular miRNA increases its range of action (Fig. 2). However, this range of action has a nonmonotonic dependence on the transport coefficient as we showed both numerically and analytically (Fig. 3). If the transport coefficient and the extracellular miRNA concentration are sufficiently large, the model predicts that the protein levels of all the recipient cells in the tissue could be below a threshold needed to trigger a cellular response (Fig. 2 and 3). The model also indicates that an increase in the transport coefficient is identical to a decrease in the rate constant of miRNA degradation (Fig. 3).

Exosomal transport can also play a role in the propagation of drug resistance in tumors.[59] The P-glycoprotein is a transmembrane protein that can be transferred by exosomes and its overexpression contributes to drug resistance in cancer cells. Our modelling approach could be used to study the propagation of drug resistance by protein-carrying exosomes, which would represent an interesting step forward in understanding how propagation phenomena can be simply studied in heterogenous tissues.

In addition, we have shown that the presence of extracellular miRNAs could act as a cell-to-cell messenger to synchronise gene expression levels of multiple cells within a cell tissue. Indeed, simulations of the model in a heterogeneous cell population, where 20% of random variation around the average value is considered for each parameter, indicate that the levels of protein output in all the cells are below the threshold needed for a cellular response if sufficient levels of extracellular miRNA are considered (Fig. 4). The results obtained for a homogeneous cell population are even more generic since they are robust to fluctuations in the parameter values and only depend on three key parameters controlling the transport and the reactivity of the microRNAs. In that context, extracellular miRNAs could be viewed as an important cell-to-cell communicator allowing for a robust homogenisation/synchronisation of the gene expression levels within the different cells of the tissue. This property could explain why cancer cells secreting aberrant levels of extracellular miRNAs can generate an oncogenic field that can modify the gene expression profile of neighbouring cells.[27]

We also showed that dynamical signatures of gene expression can also be propagated to recipient cells through extracellular miRNAs. Indeed, the secreted miRNA from a donor cell can oscillate in a periodic manner if it is embedded in a negative feedback loop (Fig. 5 and 6). The secretion of this oscillating miRNA generates sustained oscillations of its target transcripts in recipient cells, even if these transcripts are not involved in negative feedback regulations (Fig. 7). The model indicates that an increase in the transport coefficient increases the number of cells where the protein concentration oscillates but reduces the amplitude of oscillations (Fig. 8).

The role of extracellular miRNAs in the propagation of sustained oscillatory behaviours could be of particular importance for the regulation of biological rhythms such as the circadian clock. A key issue is to better understand how the circadian clock from the suprachiasmatic nucleus can be transmitted through peripheral tissues and how the 24 h-periodic oscillations of the circadian clock components can be synchronised between the cells of a tissue. In this context, the model predicts that oscillations in extracellular miRNAs could be propagated to protein output in recipient cells. As a consequence, a dynamical signature in a donor cell, here sustained oscillations, can be propagated through recipient cells, which can be crucial for cell synchronisation within a tissue. Furthermore, since the protein output in recipient cells is not directly involved in the negative feedback regulations defining the circadian clock oscillator, the model also indicates that extracellular miRNAs could considerably enlarge the oscillatory potential of numerous gene expressions within a cell tissue.[60] The latter result could explain why gene expression between cells within a tissue can be synchronised and why a relatively large proportion of transcripts are oscillating within a cell.[60,61]

Finally, we note that the content of extracellular vesicles (EVs) reflects the physiological state of their cells of origin.[16,62] It was shown that EVs and extracellular miRNAs found in body fluids may represent a promising source of biomarkers that could be specific to multiple cancers or other pathological conditions.[63,64] Numerous potential therapeutic strategies arise to counteract the effect of extracellular miRNAs that promote cancer development (oncomirs).[63,65] Indeed, one option will be to deliver exosomes containing miRNA sponges that either target the recipient cells to counteract the oncomirs, or intercept the cancer exosomes directly in the body fluids.[65] In future studies, the spatio-temporal dynamics of specific extracellular miRNAs involved in cancers could be considered. Such models would be useful complementary theoretical tools to better define the conditions leading to a reduction in the oncogenic field effect and to link the level of oncogenic biomarkers with the dynamics of gene regulatory networks involving extracellular miRNAs.

Conflicts of interest

There are no conflicts to declare.

Acknowledgements

The authors thank the ''Actions de Recherches Concertées'' program and F.R.S.-FNRS for their financial support.

References

1 D. P. Bartel, *Cell*, 2009, **136**, 215–233.
2 R. C. Friedman, K. K.-H. Farh, C. B. Burge and D. P. Bartel, *Genome Res.*, 2008, **19**, 92–105.
3 C. Xiao, D. P. Calado, G. Galler, T.-H. Thai, H. C. Patterson, J. Wang, N. Rajewsky, T. P. Bender and K. Rajewsky, *Cell*, 2007, **131**, 146–159.
4 A. M. Cheng, *Nucleic Acids Res.*, 2005, **33**, 1290–1297.
5 M.-L. Si, S. Zhu, H. Wu, Z. Lu, F. Wu and Y.-Y. Mo, *Oncogene*, 2006, **26**, 2799–2803.
6 M. J. Bueno and M. Malumbres, *Biochim. Biophys. Acta, Mol. Basis Dis.*, 2011, **1812**, 592–601.
7 M. Korpal, E. S. Lee, G. Hu and Y. Kang, *J. Biol. Chem.*, 2008, **283**, 14910–14914.
8 A. J. Giraldez, *Science*, 2005, **308**, 833–838.
9 C. Xiao and K. Rajewsky, *Cell*, 2009, **136**, 26–36.
10 D. Iliopoulos, H. A. Hirsch and K. Struhl, *Cell*, 2009, **139**, 693–706.
11 D. Iliopoulos, S. A. Jaeger, H. A. Hirsch, M. L. Bulyk and K. Struhl, *Mol. Cell*, 2010, **39**, 493–506.
12 H.-Y. M. Cheng, J. W. Papp, O. Varlamova, H. Dziema, B. Russell, J. P. Curfman, T. Nakazawa, K. Shimizu, H. Okamura, S. Impey and K. Obrietan, *Neuron*, 2007, **54**, 813–829.
13 X. Li, J. J. Cassidy, C. A. Reinke, S. Fischboeck and R. W. Carthew, *Cell*, 2009, **137**, 273–282.
14 M. S. Ebert and P. A. Sharp, *Cell*, 2012, **149**, 515–524.
15 H. Valadi, K. Ekström, A. Bossios, M. Sjöstrand, J. J. Lee and J. O. Lötvall, *Nat. Cell Biol.*, 2007, **9**, 654–659.
16 X. Chen, H. Liang, J. Zhang, K. Zen and C.-Y. Zhang, *Trends Cell Biol.*, 2012, **22**, 125–132.
17 G. Raposo and W. Stoorvogel, *J. Cell Biol.*, 2013, **200**, 373–383.
18 D. M. Pegtel, K. Cosmopoulos, D. A. Thorley-Lawson, M. A. J. van Eijndhoven, E. S. Hopmans, J. L. Lindenberg, T. D. de Gruijl, T. Wurdinger and J. M. Middeldorp, *Proc. Natl. Acad. Sci. U. S. A.*, 2010, **107**, 6328–6333.
19 N. Kosaka, H. Iguchi, Y. Yoshioka, F. Takeshita, Y. Matsuki and T. Ochiya, *J. Biol. Chem.*, 2010, **285**, 17442–17452.
20 Y. Zhang, D. Liu, X. Chen, J. Li, L. Li, Z. Bian, F. Sun, J. Lu, Y. Yin, X. Cai, Q. Sun, K. Wang, Y. Ba, Q. Wang, D. Wang, J. Yang, P. Liu, T. Xu, Q. Yan, J. Zhang, K. Zen and C.-Y. Zhang, *Mol. Cell*, 2010, **39**, 133–144.
21 C. Frühbeis, D. Fröhlich, W. P. Kuo and E.-M. Krämer-Albers, *Front. Cell. Neurosci.*, 2013, **7**, 182.
22 B. J. Goldie, M. D. Dun, M. Lin, N. D. Smith, N. M. Verrills, C. V. Dayas and M. J. Cairns, *Nucleic Acids Res.*, 2014, **42**, 9195–9208.
23 V. Zappulli, K. P. Friis, Z. Fitzpatrick, C. A. Maguire and X. O. Breakefield, *J. Clin. Invest.*, 2016, **126**, 1198–1207.
24 M. Ono, N. Kosaka, N. Tominaga, Y. Yoshioka, F. Takeshita, R. u. Takahashi, M. Yoshida, H. Tsuda, K. Tamura and T. Ochiya, *Sci. Signaling*, 2014, **7**, ra63–ra63.
25 M. Alexander, R. Hu, M. C. Runtsch, D. A. Kagele, T. L. Mosbruger, T. Tolmachova, M. C. Seabra, J. L. Round, D. M. Ward and R. M. O'Connell, *Nat. Commun.*, 2015, **6**, 7321.
26 P. D. Robbins, A. Dorronsoro and C. N. Booker, *J. Clin. Invest.*, 2016, **126**, 1173–1180.
27 S. A. Melo, H. Sugimoto, J. T. O'Connell, N. Kato, A. Villanueva, A. Vidal, L. Qiu, E. Vitkin, L. T. Perelman, C. A. Melo, A. Lucci, C. Ivan, G. A. Calin and R. Kalluri, *Cancer Cell*, 2014, **26**, 707–721.
28 N. Morozova, A. Zinovyev, N. Nonne, L.-L. Pritchard, A. N. Gorban and A. Harel-Bellan, *RNA*, 2012, **18**, 1635–1655.
29 A. Zinovyev, N. Morozova, A. N. Gorban and A. Harel-Belan, *Advances in Experimental Medicine and Biology*, Springer Nature, 2012, pp. 189–224.
30 H.-W. Kang, M. Crawford, M. Fabbri, G. Nuovo, M. Garofalo, S. P. Nana-Sinkam and A. Friedman, *PLoS One*, 2013, **8**, e53663.
31 C. Gérard, D. Gonze, F. Lemaigre and B. Novák, *PLoS Comput. Biol.*, 2014, **10**, e1003455.
32 M. Figliuzzi, E. Marinari and A. D. Martino, *Biophys. J.*, 2013, **104**, 1203–1213.
33 C. Gérard and B. Novák, *PLoS One*, 2013, **8**, e83372.
34 J. B. Gurdon and P.-Y. Bourillot, *Nature*, 2001, **413**, 797–803.
35 O. Wartlick, A. Kicheva and M. Gonzalez-Gaitan, *Cold Spring Harbor Perspect. Biol.*, 2009, **1**, a001255.
36 S. Kondo and T. Miura, *Science*, 2010, **329**, 1616–1620.
37 D. M. Richards and T. E. Saunders, *Biophys. J.*, 2015, **108**, 2061–2073.
38 R. Nagel, L. Clijsters and R. Agami, *FEBS J.*, 2009, **276**, 5447–5455.
39 D. Gatfield, G. L. Martelot, C. E. Vejnar, D. Gerlach, O. Schaad, F. Fleury-Olela, A.-L. Ruskeepaa, M. Oresic,

C. C. Esau, E. M. Zdobnov and U. Schibler, *Genes Dev.*, 2009, **23**, 1313–1326.
40 V. R. Shende, M. M. Goldrick, S. Ramani and D. J. Earnest, *PLoS One*, 2011, **6**, e22586.
41 E. Levine, P. McHale and H. Levine, *PLoS Comput. Biol.*, 2007, **3**, e233.
42 S. Hock, Y.-K. Ng, J. Hasenauer, D. Wittmann, D. Lutter, D. Trümbach, W. Wurst, N. Prakash and F. J. Theis, *BMC Syst. Biol.*, 2013, **7**, 48.
43 A. Mugler, A. Levchenko and I. Nemenman, *Proc. Natl. Acad. Sci. U. S. A.*, 2016, **113**, E689–E695.
44 R. Beckerman and C. Prives, *Cold Spring Harbor Perspect. Biol.*, 2010, **2**, a000935.
45 S. P. Gygi, Y. Rochon, B. R. Franza and R. Aebersold, *Mol. Cell. Biol.*, 1999, **19**, 1720–1730.
46 U. Bissels, S. Wild, S. Tomiuk, A. Holste, M. Hafner, T. Tuschl and A. Bosio, *RNA*, 2009, **15**, 2375–2384.
47 B. Schwanhäusser, D. Busse, N. Li, G. Dittmar, J. Schuchhardt, J. Wolf, W. Chen and M. Selbach, *Nature*, 2011, **473**, 337–342.
48 T. Tian, Y.-L. Zhu, F.-H. Hu, Y.-Y. Wang, N.-P. Huang and Z.-D. Xiao, *J. Cell. Physiol.*, 2013, **228**, 1487–1495.
49 A. C. Romano, E. M. Espana, S. H. Yoo, M. T. Budak, J. M. Wolosin and S. C. G. Tseng, *Invest. Opthalmol. Vis. Sci.*, 2003, **44**, 5125.
50 M. Shipitsin, L. L. Campbell, P. Argani, S. Weremowicz, N. Bloushtain-Qimron, J. Yao, T. Nikolskaya, T. Serebryiskaya, R. Beroukhim, M. Hu, M. K. Halushka, S. Sukumar, L. M. Parker, K. S. Anderson, L. N. Harris, J. E. Garber, A. L. Richardson, S. J. Schnitt, Y. Nikolsky, R. S. Gelman and K. Polyak, *Cancer Cell*, 2007, **11**, 259–273.
51 B. Bonev, P. Stanley and N. Papalopulu, *Cell Rep.*, 2012, **2**, 10–18.
52 R. Chen, M. D'Alessandro and C. Lee, *Curr. Biol.*, 2013, **23**, 1959–1968.
53 M. Osella, C. Bosia, D. Corá and M. Caselle, *PLoS Comput. Biol.*, 2011, **7**, e1001101.
54 Y. Li, Y. Li, H. Zhang and Y. Chen, *PLoS One*, 2011, **6**, e26302.
55 J. Tsang, J. Zhu and A. van Oudenaarden, *Mol. Cell*, 2007, **26**, 753–767.
56 K. Ohshima, K. Inoue, A. Fujiwara, K. Hatakeyama, K. Kanto, Y. Watanabe, K. Muramatsu, Y. Fukuda, S. Ogura, K. Yamaguchi and T. Mochizuki, *PLoS One*, 2010, **5**, e13247.
57 R. S. Redis, S. Calin, Y. Yang, M. J. You and G. A. Calin, *Pharmacol. Ther.*, 2012, **136**, 169–174.
58 M. Alečković and Y. Kang, *Biochim. Biophys. Acta, Rev. Cancer*, 2015, **1855**, 24–42.
59 M. M. Lv, X. Y. Zhu, W. X. Chen, S. L. Zhong, Q. Hu, T. F. Ma, J. Zhang, L. Chen, J. H. Tang and J. H. Zhao, *Tumor Biol.*, 2014, 10773–10779.
60 R. Zhang, N. F. Lahens, H. I. Ballance, M. E. Hughes and J. B. Hogenesch, *Proc. Natl. Acad. Sci. U. S. A.*, 2014, **111**, 16219–16224.
61 K. L. Eckel-Mahan, V. R. Patel, R. P. Mohney, K. S. Vignola, P. Baldi and P. Sassone-Corsi, *Proc. Natl. Acad. Sci. U. S. A.*, 2012, **109**, 5541–5546.
62 M. Yáñez-Mó, P. R.-M. Siljander, Z. Andreu, A. B. Zavec, F. E. Borràs, E. I. Buzas, K. Buzas, E. Casal, F. Cappello, J. Carvalho, E. Colás, A. C. da Silva, S. Fais, J. M. Falcon-Perez, I. M. Ghobrial, B. Giebel, M. Gimona, M. Graner, I. Gursel, M. Gursel, N. H. H. Heegaard, A. Hendrix, P. Kierulf, K. Kokubun, M. Kosanovic, V. Kralj-Iglic, E.-M. Krämer-Albers, S. Laitinen, C. Lässer, T. Lener, E. Ligeti, A. Liñe, G. Lipps, A. Llorente, J. Lötvall, M. Manček-Keber, A. Marcilla, M. Mittelbrunn, I. Nazarenko, E. N. N. 't Hoen, T. A. Nyman, L. O. Driscoll, M. Olivan, C. Oliveira, É. Pállinger, H. A. del Portillo, J. Reventós, M. Rigau, E. Rohde, M. Sammar, F. Sánchez-Madrid, N. Santarém, K. Schallmoser, M. S. Ostenfeld, W. Stoorvogel, R. Stukelj, S. G. V. der Grein, M. H. Vasconcelos, M. H. M. Wauben and O. D. Wever, *J. Extracell. Vesicles*, 2015, **4**, 27066.
63 S. Pant, H. Hilton and M. E. Burczynski, *Biochem. Pharmacol.*, 2012, **83**, 1484–1494.
64 L. Li, D. Masica, M. Ishida, C. Tomuleasa, S. Umegaki, A. N. Kalloo, C. Georgiades, V. K. Singh, M. Khashab, S. Amateau, Z. Li, P. Okolo, A.-M. Lennon, P. Saxena, J.-F. Geschwind, T. Schlachter, K. Hong, T. M. Pawlik, M. Canto, J. Law, R. Sharaiha, C. R. Weiss, P. Thuluvath, M. Goggins, E. J. Shin, H. Peng, V. Kumbhari, S. Hutfless, L. Zhou, E. Mezey, S. J. Meltzer, R. Karchin and F. M. Selaru, *Hepatology*, 2014, **60**, 896–907.
65 E. Anastasiadou and F. J. Slack, *Science*, 2014, **346**, 1459–1460.